Proceedings of IMECE'02
2002 ASME International Mechanical Engineering Congress and Exposition
November 17-22, 2002, New Orleans, Louisiana, USA

IMECE02/HT-32124

MONTE CARLO MODELING OF HEAT GENERATION IN ELECTRONIC NANOSTRUCTURES

Eric Pop
Dept. of Electrical Engineering
Stanford University
Stanford, CA 94305
Email: epop@stanford.edu

Sanjiv Sinha
Dept. of Mechanical Engineering
Stanford University
Stanford, CA 94305
Email: sanjiv@stanford.edu

Kenneth E. Goodson
Dept. of Mechanical Engineering
Stanford University
Stanford, CA 94305
Email: goodson@stanford.edu

ABSTRACT

This work develops a Monte Carlo (MC) simulation method for calculating the heat generation rate in electronic nanostructures. Electrons accelerated by the electric field scatter strongly with optical phonons, yet heat transport in silicon occurs via the faster acoustic modes. The MC method incorporates the appropriate energy transfer rates from electrons to each phonon branch. This accounts for the non-equilibrium energy exchange between the electrons and phonon branches. Using the MC method with an electron energy-dependent scattering rate intrinsically accounts for the non-locality of the heat transfer near a strongly peaked electric field. This approach provides more information about electronically generated heat at nanoscale dimensions compared to traditional macroscopic field-dependent methods. The method has applications in any region of high spatial or temporal non-equilibrium between electrons and phonons, and particularly facilitates careful microscopic analysis of heating in a nanoscale transistor.

NOMENCLATURE

Λ phonon mean free path
C_s heat capacity per unit volume
k_s thermal conductivity
T lattice temperature
Q''' heat generation rate per unit volume
τ_{ph} phonon-phonon scattering time
u phonon energy density per unit volume and unit solid angle
u_o equilibrium phonon energy density
$\mathbf{v}$ phonon velocity
$\mathbf{J}$ electron current density
$\mathbf{E}$ electric field
LA longitudinal acoustic
TA transverse acoustic
LO longitudinal optical
TO transverse optical
$\hbar$ Planck's constant divided by 2π
$\mathbf{k}$ electron wave vector
$\Gamma(\mathbf{k})$ electron-phonon scattering rate
$M(\mathbf{k})$ electron-phonon matrix element
$E_{\mathbf{k}}$ electron energy
$g(E_{\mathbf{k}})$ electron density of states
ω_q phonon frequency
m^* electron effective mass
$\mathbf{p}'$ electron momentum after a scattering event

INTRODUCTION

Understanding heat generation and conduction at nanoscales has become important in the context of short-pulse laser heating, thin films and integrated circuits. In silicon-on-insulator (SOI) circuit technology, for example, transistors are built in a thin silicon film which rests on top of a thicker silicon dioxide layer. This allows faster switching speeds of SOI transistors due to less capacitive coupling with the substrate. Even thinner silicon layers are desirable to further reduce parasitic capacitances and to increase gate control of the transistor body. Unfortunately the silicon dioxide layer has poor thermal conductivity so most heat

Copyright © 2002 by ASME

generated during device operation is confined to the thin silicon film. As transistor dimensions and the silicon film thickness are scaled to the order of tens of nanometers, i.e. much less than the phonon mean free path ($\Lambda \approx 300$ nm in bulk silicon at room temperature), sub-continuum effects are expected to become important. Phonon boundary scattering [1] and phonon confinement effects [2] are known to decrease the effective thermal conductivity of thin silicon films. When the dimensions of the heat source become smaller than Λ, ballistic phonon emission effects must also be accounted for [3]. Nanoscale heat conduction measurements are very difficult to perform, therefore simulations play an increasingly important role in understanding heat generation and transfer at such small scales.

The continuum classical heat diffusion equation

$$C_s \frac{\partial T}{\partial t} = \nabla \cdot (k_s \nabla T) + Q''' \quad (1)$$

cannot properly resolve heat transfer problems on small time scales (on the order of the phonon relaxation times, i.e. picoseconds) or short length scales (nanometers, or less than Λ). Continuum heat transport theory must therefore be replaced by a more sophisticated formulation which takes into account the "granularity" of heat transfer — i.e. energy transport via lattice wave packets, also known as phonons. At length scales less than Λ but larger than the phonon wavelength phonons can be treated as particles and the Boltzmann Transport Equation (BTE) may be used, written here in a transformed form as [4]:

$$\frac{\partial u}{\partial t} + \mathbf{v} \cdot \nabla u = \frac{u_o - u}{\tau_{ph}} + Q''' \quad (2)$$

where u is the phonon energy density and $\mathbf{v}$ is the average phonon velocity (assumed isotropic). Yet irrespective of the complexity of the phonon transport model, the problem still strongly depends on identifying a proper model for the Joule heating source term from electron-phonon interactions, Q'''.

EVALUATING THE HEATING RATE

In electronic nanostructures such as transistors, the nearly-free conduction band electrons are accelerated by the electric field. The electrons gain energy from the field, then lose it by scattering with the lattice phonons [5]. The lattice absorbs the extra electron energy, heats up and in turn, affects the electronic transport properties of the material. These processes are symbolically illustrated in Fig. 1. The dotted lines represent the effect the phonons have on the electron population and hence, their transport: electron mobility in bulk silicon decreases with the temperature rise roughly as $T^{-2.4}$ around room temperature.

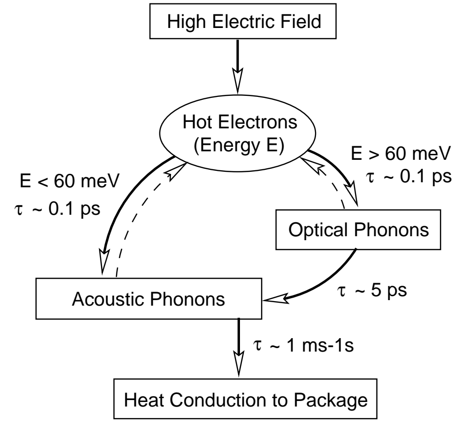

Figure 1. Diagram and characteristic time scales of the energy transfer processes in silicon. Scattering with low group velocity optical phonons is the dominant relaxation mechanism for electron energies above 60 meV. This creates a phonon energy bottleneck until the optical phonons decay into the faster acoustic modes.

Energetic electrons scatter strongly with the optical phonon branches which have relatively low group velocity, on the order of 1000 m/s. However, the primary heat carriers in silicon are the faster acoustic phonon modes, with group velocities around 8-9000 m/s (the group velocity of a phonon branch is given by its slope on the dispersion relationship from Fig. 2). Optical phonons decay into acoustic phonons, but over relatively long time scales (picoseconds) compared to the electron-optical phonon scattering time (on the order of tenths of picoseconds). This creates a phonon energy bottleneck which can lead the energy and density of optical phonon modes to build up over time, further impeding the electron transport.

The current state of the art heat transport simulations replace the heat diffusion equation with various solutions of the phonon Boltzmann Transport Equation. Mazumder [6] solved the BTE with the Monte Carlo (MC) method but only considered the acoustic phonon branches, hence forsaking direct applicability of the method to the electronically-generated heat in transistors. Sverdrup [4] solved the phonon BTE (both for the acoustic and optical phonons) via the finite volume method inside a transistor, but assumed all electron energy was dissipated to the optical phonon modes which were approximated as perfectly stationary (hence exaggerating the phonon energy bottleneck previously mentioned). As with other previous publications, Sverdrup [4] also modeled the Joule heating term as the dot product of the *macroscopic* electric field and current density:

$$Q''' = \mathbf{J} \cdot \mathbf{E} \quad (3)$$

Unfortunately, such an approach cannot account for the *microscopic* non-locality of the heat generation near a strongly peaked

Copyright © 2002 by ASME

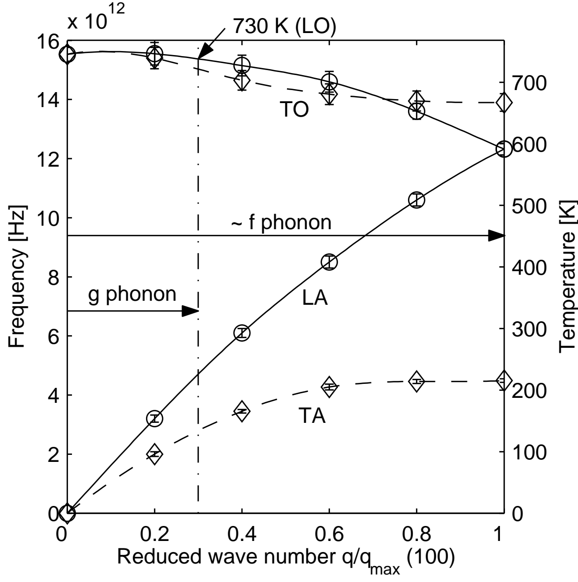

Figure 2. Phonon dispersion relationship in silicon along the (100) direction, based on neutron scattering data [7]. The f and g phonons are involved in the intervalley scattering of electrons [8]. The 730 K LO phonon is thought to dominate optical phonon scattering for electrons with energies above 60 meV.

field region: although electrons gain most of their energy at the location of the peak electric field, they typically travel another electron-phonon mean free path before releasing their energy to the lattice. Assuming an electron velocity of 10^7 cm/s (the saturation velocity in silicon) and an electron-phonon scattering time around 0.1 ps, the electron-phonon mean free path in silicon is about 10 nm. While such a small discrepancy may be neglected on length scales of microns, or even tenths of a micron, it ought to be taken into account when simulating heat generation rates on smaller length scales — for example, within a 10-20 nm future generation transistor. In addition, the macroscopic formulation of Eq. (3) also does not differentiate between electron energy exchange with optical versus acoustic phonons.

The present work addresses both issues outlined above: we present a methodology for extracting sub-continuum phonon branch-specific heat generation rates directly from an electron MC simulator, with applications at nanometer length scales.

FORMULATION

Electron-Phonon Scattering

Conduction band electrons in silicon can scatter with each other, with impurities, crystal imperfections, boundaries or with the silicon lattice phonons. Among these mechanisms, electrons only lose energy by scattering with lattice phonons. The other mechanisms are thought to only affect the electron momentum [5]. Joule heating of the silicon lattice occurs precisely through the mechanism of electron-phonon scattering.

The electron-phonon scattering rate is typically computed from Fermi's Golden Rule as [9]:

$$\Gamma(\mathbf{k}) = \frac{2\pi}{\hbar} \mid M(\mathbf{k}) \mid^2 g(E_k \pm \hbar\omega_q) \tag{4}$$

and it increases roughly with the square root of electron energy, like the electron density of states, $g(E)$ in 3-D. The matrix element $M(\mathbf{k})$ includes the dependence on the phonon occupation of states, on the wave function overlap integral and on the deformation potential characteristic of the particular phonon involved. Deformation potential values are typically extracted from comparison with low and high temperature electron mobility data [10].

In silicon, optical phonons have a minimum cut-off frequency just over 12 THz, corresponding to an equivalent temperature of 600 K, as shown in the dispersion relationship of Fig. 2. Electrons with energies less than the minimum optical phonon energy can only absorb (not emit) optical phonons. Hence, scattering and energy relaxation of low energy electrons is dominated by acoustic phonons, particularly the longitudinal branch. It can be shown [9] that a single isotropic deformation potential of 9 eV is sufficient to describe scattering with both LA and TA phonons. The "lumped" acoustic phonon velocity is typically taken to be 9000 m/s, the value of the LA phonon group velocity near the Brillouin zone center. In fact, intravalley scattering (within the same conduction band valley) is almost entirely dominated by acoustic phonons because intravalley scattering with optical phonons is forbidden to first order [9].

Hot electrons with energies above the optical phonon energy scatter most effectively with the 730 K longitudinal optical (LO) phonon in silicon [8]. This phonon, located at 0.3 of the Brillouin zone edge in the phonon dispersion relationship (Fig. 2), satisfies the momentum conservation rule for intervalley scattering between conduction band valleys on the same axis, e.g. from (100) to (-100). This phonon is often referred to as a g-phonon and this intervalley transfer is called g-type scattering [8]. These LO phonons have small group velocities, around 1000 m/s, and are relatively stationary in the hot spot region where they are formed. They anharmonically decay into the faster acoustic phonons which in turn transport the energy out. Another type of intervalley transfer can occur between conduction band valleys on perpendicular axes, e.g. from (100) to (010) or (001). The optical phonon required to conserve momentum in this process is the TO f-type phonon shown in Fig. 2. This phonon has an energy of 59 meV, while the g-type LO phonon has an energy of 63 meV. The small separation of these energies has made it hard to distinguish between their effects in comparison with mobility data, leading to some scientific disagreement regarding their relative strengths [11, 12]. In this work we group these

Copyright © 2002 by ASME

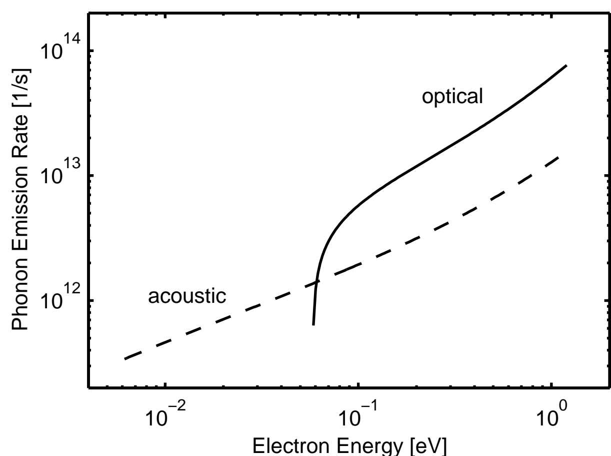

Figure 3. Phonon emission rates as a function of electron energy as computed from Eq. (4). Note the strong onset of electron-optical phonon scattering for electrons with energies above 60 meV.

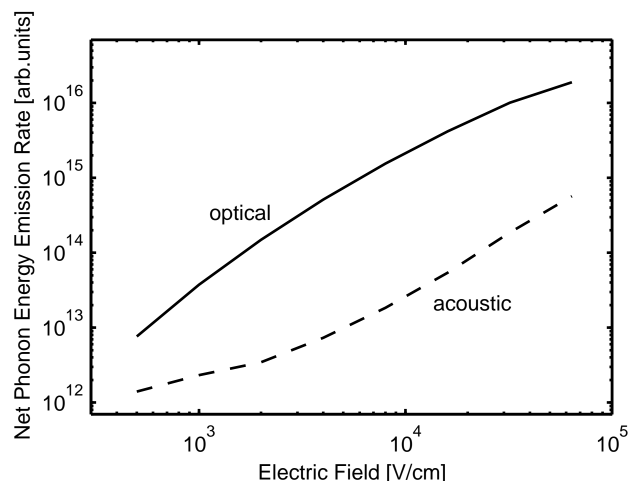

Figure 4. Net (emission less absorption) energy generation rates for optical and acoustic phonons at practical steady-state electric fields.

phonons together and consider intervalley scattering with a single optical phonon of 60 meV and a single deformation potential value (1.25×10^9 eV/cm) chosen to fit Canali's [10] experimental bulk mobility data. Figure 3 plots the phonon emission rates as a function of electron energy, for both acoustic and optical phonons, using the scattering parameters adopted in this work.

Monte Carlo Implementation

We have implemented an electron Monte Carlo simulator set up in such a way as to facilitate the collection of information about phonon scattering events. Otherwise, the method followed is consistent with the one described by [5] and [11]. In brief, this can be summarized as follows: several tens of thousands electrons are initialized with thermal energy distributions. Each particle can be individually followed throughout the simulation. For each electron, a random number is drawn to determine its time of free flight. During this time the particle is allowed to drift under the influence of the electric field as dictated by Newton's laws of motion. Then another random number is drawn and compared with pre-computed cumulative probabilities of scattering. A scattering event (e.g. with impurities, acoustic or optical phonons) is selected in proportion to the strength of each process. A non-scattering event (often called "self-scattering") can also be selected, in which case the particle continues its free flight unimpeded. If a real scattering process is selected the particle's energy and momentum are adjusted as necessary and another random time of flight is drawn. In our simulator, all phonon emission and absorption events are also tallied at this point. The procedure then repeats until enough statistics are gathered.

Electron energy bands in the non-parabolic approximation (with non-parabolicity parameter $\alpha = 0.5$ eV^{-1}) were used. Care was taken in implementing inelastic scattering with acoustic phonons as in [11]. Numerous other Monte Carlo studies treat acoustic scattering as purely elastic (i.e. no energy is exchanged in the process) — but this cannot be assumed here, as we are specifically interested in how the acoustic phonon heat is generated. The acoustic phonon mode dispersion was assumed to be linear with group velocity 9000 m/s, which is the LA phonon group velocity near the Brillouin zone center. This is justified, as most acoustic phonon scattering occurs with LA phonons of small wave vector. Optical phonon scattering was modeled with a single optical phonon at 60 meV as described in the previous section. Consequently, with each optical emission (or absorption) event electrons lose (or gain) 60 meV of energy and an equivalent phonon is generated and tallied. Phonon scattering is typically considered isotropic and the direction of the momentum of each electron after a collision is chosen at random in 3-D. The magnitude of the electron momentum after an interaction with a phonon reflects the energy lost or gained:

$$|\,\mathbf{p}'\,| = \sqrt{2m^*(E \pm \hbar\omega_q)} \tag{5}$$

where the plus sign corresponds to a phonon absorption and minus to a phonon emission.

Our Monte Carlo simulator can be used in zero, one and two dimensions. In "zero" dimensions it computes all electron and phonon energies within a one micron section of an infinite silicon resistor (simulated with periodic boundary conditions). In one or two dimensions it is best used as a post-processor for other electron device solvers. The potentials and carrier distributions from other (simpler, but faster) commercially available programs can be input as initial conditions for the most time-efficient use

Copyright © 2002 by ASME

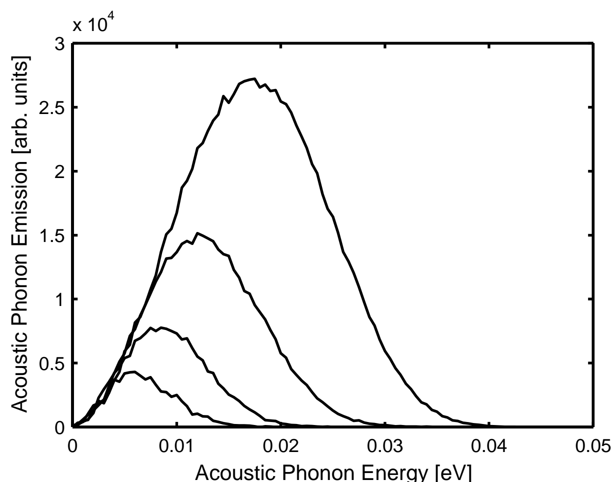

Figure 5. Net (emission less absorption) acoustic phonon generation rate distribution as a function of phonon energy, for steady-state applied electric fields of 10, 20, 40 and 80 kV/cm, from bottom to top curves.

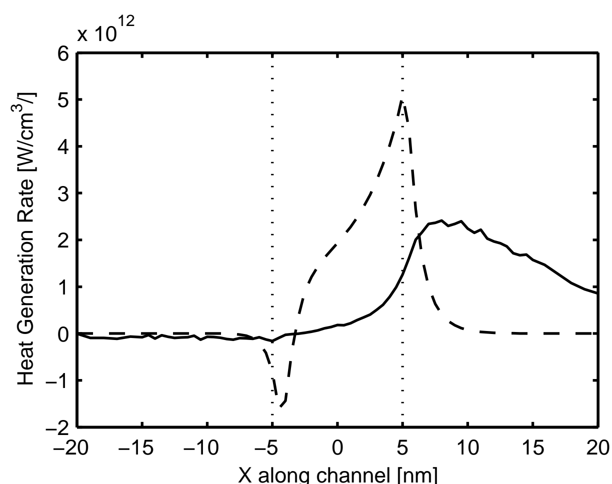

Figure 6. Heat generation profile along the channel of a possible 10 nm SOI MOSFET. The dashed line represents the heating rate obtained from the conventional macroscopic Eq. (3), the solid line is the heating profile obtained with our MC simulations. The source and drain are to the left and right, respectively, of the vertical dotted lines.

of our MC code. The outputs we are specifically interested in are the relative phonon (optical and acoustic) generation rates and their localization within a physical silicon device.

RESULTS

Incorporating electron scattering events into the Monte Carlo scheme implicitly accounts for the heat dissipation rates into the various phonon branches. The net heat generation rates can be easily obtained as the sum of all phonon emission events minus all phonon absorption events divided by the total simulation time. The phonon branch-specific results (acoustic versus optical) are displayed in Fig. 4, at several steady-state electric fields applied along our "infinite" resistor. As expected, Joule heating of the optical phonon modes dominates acoustic mode heating by approximately an order of magnitude for most practical electric field values. The optical phonons eventually decay into acoustic phonons with higher group velocities which transport heat to the contacts and out of the electronic device.

The more complete breakdown of the generated acoustic phonon energies is shown in Fig. 5. The distributions are shown at four different steady-state electric field values, within the typical operating range of an electron device. Low energy phonon generation vanishes with the phonon density of states as the phonon energy approaches zero. The distribution is limited at higher phonon energies by the diminishing number of hot electrons which are available to emit the higher energy acoustic modes and the predominance of optical phonon emission. These limits give the acoustic phonon distribution its bell-shaped form. Note that the average energy of the net emitted acoustic phonons in Fig. 5 are 6.9, 9.3, 12.9 and 17.7 meV, corresponding to 1.67, 2.25, 3.12 and 4.28 THz frequencies of the LA phonon branch.

Applications

Careful accounting of the electron-phonon interaction and the various phonon modes is especially relevant in the sub-continuum limit, i.e. at dimensions less than the electron and phonon mean free path. This is of particular importance in evaluating the self-heating phenomena expected to occur in transistors at the scaling limits of silicon device technology, at 10-20 nm channel lengths.

We have applied our MC simulator to the 10 nm dual-gate SOI (DGSOI) transistor proposed by Lundstrom [13]. Compared to today's commercially-available transistor technology (with gate lengths around 180 nm), such a transistor is thought to represent the theoretical scaling limit of silicon devices. Aside from tremendous and still unresolved fabrication issues, large leakage currents due to quantum tunneling are generally believed to render any smaller transistors unusable.

"Sub-continuum," ballistic transport is expected to dominate both electron and heat conduction within a 10 nm DGSOI device. The transport is also expected to be one-dimensional, along the thin SOI layer. We used the nanoMOS 2.0 simulator [14] to extract the carrier and electric field distributions inside the proposed device at gate and drain voltages of 0.6 Volts. These distributions were input into our Monte Carlo program, which was run as a post-processor until steady-state was achieved and enough statistics were gathered. The resulting heat generation profiles along the channel of the transistor are shown in Fig. 6. The dis-

Copyright © 2002 by ASME

crepancy between use of the traditional method of computing the heating rate (Eq. (3) and the dashed line in Fig. 6) and the Monte Carlo results is particularly evident at such small scales. Electrons are injected almost ballistically across the short channel and they release most of their energy to the lattice phonons just inside the drain. The peak heating rate predicted by MC occurs a few nanometers inside the drain, "downstream" from the peak of the electric field. The shape of the MC heat generation rate is also different: electrons lose energy more gradually (on the order of 60 meV per scattering length, or every few nanometers) than predicted by Eq. (3), where the electric field sharply drops to zero in the highly doped drain. Negative heat generation regions correspond to net energy absorption from the lattice: electrons in the source absorb more phonons than they emit as the high-energy tail of their distribution surmounts the barrier of injection into the channel. The "traditional" method of simulating Q''' as the dot product of the electric field and the current density is clearly inadequate at such small scales. Use of the MC method is essential because it properly captures the non-equilibrium electron distribution just inside the drain region where most of the device heating occurs. The region just inside the drain is a mixture of hot electrons injected almost ballistically across the channel and thermal electrons already present due to the high doping levels and the vicinity of the contact.

The energy released by the injected electrons creates an effective phonon "hot spot" just inside the drain. The proximity of this hot spot to the transistor's source (also the source of conduction electrons), i.e. nearly within an optical phonon decay length, may allow a considerable number of hot optical phonons to travel to the source and affect the electron injection there. Any perturbation on the electron injection velocity at the source is thought to ultimately affect the current drive of the transistor [5]. This phenomena has been previously estimated [15] but not yet quantized within a rigorous Monte Carlo scheme. Such work remains to be done.

CONCLUSIONS

The Monte Carlo method was used to compute heat generation in silicon at nanoscales. This approach gives direct information on the magnitude and types of phonons that are generated through electronic Joule heating in semiconductor nanostructures. Distinction is implicitly made between the phonon modes receiving most of the heat (optical) and those responsible for most of the heat transport (acoustic). The MC method also provides more accurate spatial information about the localization of the heat source, particularly at length scales less than the phonon and electron mean free path. The knowledge can be used to resolve the exact magnitude and source of heating within a nanoscale transistor. The generated phonon distributions may be used as an input to a phonon Monte Carlo simulator.

ACKNOWLEDGMENT

The authors wish to thank the Semiconductor Research Corporation (SRC) task 751.001 for sponsoring this research. Eric Pop is supported by the SRC/IBM Graduate Fellowship. Sanjiv Sinha is supported by the Stanford Graduate Fellowship.

REFERENCES

[1] Asheghi, M., Leung, Y., Wong, S. and Goodson, K.E., "Phonon-boundary scattering in thin silicon layers," *Applied Physics Letters*, vol. 71, pp. 1798-1800, 1997

[2] Balandin, A. and Wang, K.L., "Significant decrease of the lattice thermal conductivity due to phonon confinement in a free-standing semiconductor quantum well," *Physical Review B*, vol. 58, pp. 1544-1549, 1998

[3] Sverdrup, P., Sinha, S., Asheghi, M., Uma, S. and Goodson, K.E., "Measurement of ballistic phonon conduction near hotspots in silicon," *Applied Physics Letters*, vol. 78, p. 3331-3333, 2001

[4] Sverdrup, P., Ju, Y.S. and Goodson, K.E., "Sub-continuum simulations of heat conduction in silicon-on-insulator transistors," *Journal of Heat Transfer*, vol. 123, pp. 130-137, 2001

[5] Lundstrom, M., *Fundamentals of Carrier Transport*, 2nd Edition, Cambridge University Press, 2000

[6] Mazumder, S. and Majumdar, A., "Monte Carlo study of phonon transport in solid thin films including dispersion and polarization," *J. of Heat Transfer*, vol. 123, pp. 749-759, 2001

[7] Dolling, G., "Lattice vibrations in crystals with the diamond structure," *Symposium on Inelastic Scattering of Neutrons in Solids and Liquids*, pp. 37-48, 1963

[8] Long, D., "Scattering of conduction electrons by lattice vibrations in silicon," *Physical Review*, vol. 120, p. 2024, 1960

[9] Ferry, D.K., *Semicond. Transport*, Taylor & Francis, 2000

[10] Canali, C, Jacoboni, C., Nava, F., Ottaviani, G. and Alberigi-Quaranta, A., "Electron drift velocity in silicon," *Physical Review B*, vol. 12, pp. 2265-2283, 1975

[11] Jacoboni, C. and Reggiani., L., "The Monte Carlo method for the solution of charge transport in semiconductors with applications to covalent materials," *Reviews of Modern Physics*, vol. 55, pp. 645-705, 1983

[12] Yamada, T., Zhou, J.-R., Miyata, H. and Ferry, D.K., "In-plane transport properties of $Si/Si_{1-x}Ge_x$ structure and its FET performance by computer simulation," *IEEE Transactions on Electron Devices*, vol. 41, pp. 1513-1522, 1994

[13] Lundstrom, M. and Ren, Z., "Essential physics of carrier transport in nanoscale MOSFETs," *IEEE Transactions on Electron Devices*, vol. 49, pp. 133-141, 2002

[14] http://www.ece.purdue.edu/celab

[15] Pop, E., Banerjee, K., Dutton, R. and Goodson, K.E., "Localized heating effects and scaling of sub-0.18 micron CMOS devices," *International Electron Devices Meeting 2001*, IEDM Technical Digest, pp. 31.1.1-31.1.4

Copyright © 2002 by ASME